THEMIS observations of long-lived regions of large-amplitude whistler waves in the inner magnetosphere

C. M. Cully,[1,2] J. W. Bonnell,[3] and R. E. Ergun[4]

Received 14 February 2008; revised 17 April 2008; accepted 24 April 2008; published 10 June 2008.

[1] Recent reports of large-amplitude whistler waves (>100 mV/m) in the radiation belts have intensified interest in the role of whistler waves in accelerating radiation belt electrons to MeV energies. Several critical parameters for addressing this issue have not previously been observed, including the occurrence frequency, spatial extent and longevity of regions of large-amplitude whistlers. The THEMIS mission, with multiple satellites in a near-equatorial orbit, offers an excellent opportunity to study these waves. We use data from the Electric Field Instrument (EFI) to show that in the dawn-side radiation belts, especially near L-shells from 3.5 to 5.5, the probability distribution of wave activity has a significant high-amplitude tail and is hence not well-described by long-term time averages. Regions of enhanced wave activity exhibit four-second averaged wave power above 1 mV/m and sub-second bursts up to several hundred mV/m. These regions are spatially localized to at most several hours of local time azimuthally, but can persist in the same location for several days. With large regions of space persistently covered by bursty, large-amplitude waves, the mechanisms and rates of radiation belt electron acceleration may need to be reconsidered.
Citation: Cully, C. M., J. W. Bonnell, and R. E. Ergun (2008), THEMIS observations of long-lived regions of large-amplitude whistler waves in the inner magnetosphere, *Geophys. Res. Lett.*, *35*, L17S16, doi:10.1029/2008GL033643.

1. Introduction

[2] Physical processes working in the outer Van Allen radiation belts can both accelerate particles to MeV energies and also rapidly drain the resulting energetic populations. Several acceleration mechanisms are known, including impulsive changes in the large-scale magnetic field configuration [*Li et al.*, 2001], drift-resonant interaction with Ultra-Low Frequency (ULF) waves [*Elkington et al.*, 2003; *Mann et al.*, 2004] and Doppler-shifted cyclotron-resonant interactions with whistler-mode waves [*Horne and Thorne*, 2003; *Meredith et al.*, 2003]. Since all of these acceleration mechanisms tend to be active simultaneously with a still-longer list of depletion mechanisms, the response of the system to its solar wind drivers is non-trivial [*Onsager et al.*, 2007].

[3] Observations by *Santolk et al.* [2003] of >30 mV/m parallel-propagating whistler-mode waves, and by *Cattell et al.* [2008] of >250 mV/m oblique whistlers, suggest a new paradigm for acceleration by whistler waves. Rather than being gradually energized by repeated interactions with weak waves (on the order 0.1 mV/m), radiation belt electrons may be abruptly accelerated by relatively few interactions with extremely intense waves. At such large amplitudes, nonlinear wave-particle interaction effects including phase trapping become important, and can accelerate particles to relativistic energies [*Omura et al.*, 2007; *Summers and Omura*, 2007]. Simulations of electrons interacting with order 100 mV/m whistler waves show acceleration to MeV energies in as little as 0.1 s [*Cattell et al.*, 2008]. In order to quantitatively assess the role these waves play in radiation belt dynamics, several observational issues need to be addressed, including the occurrence frequency and amplitude distribution of the waves, and the spatial and temporal extent of the regions in which they are found.

[4] The THEMIS mission [*Angelopoulos*, 2008] consists of 5 satellites in near-equatorial orbits with apogees above 10 Earth radii (R_E) and perigees below 2 R_E. Equipped with high-quality fields instruments, these satellites offer an excellent opportunity to study the characteristics of large-amplitude whistler waves in relevant regions of space. In this paper, we present the first observations of large-amplitude whistler waves from the THEMIS Electric Fields Instrument (EFI).

2. Wave Power Statistics

[5] The Digital Fields Board (DFB) (C. M. Cully et al., The THEMIS digital fields board, submitted to *Space Science Reviews*, 2008) calculates the mean amplitude of the electric and magnetic fields in 6 logarithmically-spaced passbands up to 4 kHz using electric field data from the double-probe Electric Fields Instrument (EFI) (J. Bonnell et al., The electric field experiment on the THEMIS satellites, submitted to Space Science Reviews, 2008) and magnetic field data from the Search Coil Magnetometer (SCM) (A. Roux et al., The search coil magnetometer for THEMIS, submitted to *Space Science Reviews*, 2008). The resulting amplitude values (filter bank data) are included in the survey mode telemetry, covering most orbits with a measurement cadence of four seconds. The EFI booms on probes C, D and E were deployed in the early summer of 2007; with near-continual coverage on three probes in near-equatorial orbits, the filter bank data from these instruments provide a solid foundation for a statistical analysis of wave power. The booms on the two remaining probes have now

[1]Laboratory for Atmospheric and Space Physics, University of Colorado, Boulder, Colorado, USA.
[2]Now at Swedish Institute of Space Physics, Uppsala, Sweden.
[3]Space Sciences Laboratory, University of California, Berkeley, California, USA.
[4]Laboratory for Atmospheric and Space Physics, University of Colorado, Boulder, Colorado, USA.

0094-8276/08/2008GL033643$05.00

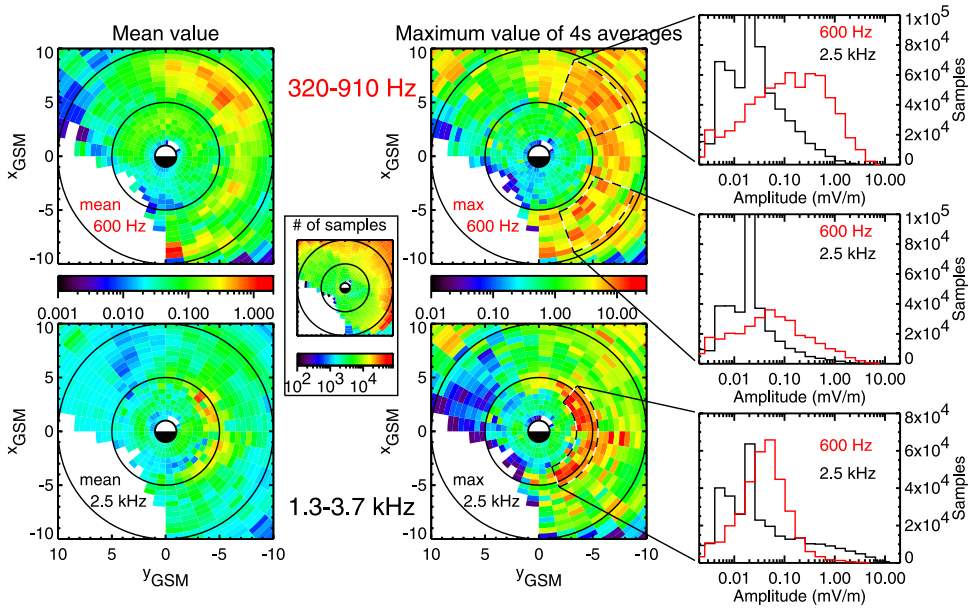

Figure 1. Wave amplitudes in mV/m from the filter bank data on THEMIS C, D and E. (left) Mean amplitude as a function of position in the GSM plane in the (top) 600 Hz band and (bottom) 2.5 kHz band. Inset: number of filter bank spectra used in each cell in the left and middle plots. (middle) Maximum value of the four-second averaged filter bank data. (right) Histograms of the filter bank values in the regions shown.

been successfully deployed, and we expect 5-probe coverage for 2008.

[6] Between June and December 2007, there are a combined 73 million electric field filter bank spectra from probes C, D and E after removing bad data intervals (telemetry errors, intervals when the EFI was operating in diagnostic or non-optimal modes, spacecraft thruster firings, etc.). The leftmost plots of Figure 1 show the mean value of these data as binned by location in the xy plane in Geocentric Solar Magnetic (GSM) coordinates. The top left plot displays mean power in the 600 Hz band (320 to 910 Hz), while mean power in the 2.5 kHz band (1.3 kHz to 3.7 kHz) is shown at the bottom left.

[7] The upper whistler band, from 0.5 to 1.0 times the electron cyclotron frequency, overlaps with the 2.5 kHz band near 5 R_E, and with the 600 Hz band near 8 R_E. Localized intensity peaks exist at these distances on the dawn side in the corresponding frequency band. The mean amplitudes reach 1 to 2 mV/m in these enhanced regions, consistent with the results of *Meredith et al.* [2001] based on CRRES data.

[8] Although the mean value has interest in and of itself, the radiation belt particles may be energized by relatively rare large-amplitude events, rather than frequent low-amplitude events. To investigate such large-amplitude waves, we first plot the maximum value of the (four-second averaged) filter bank data as a function of position in the middle plots of Figure 1. The dawn sector again exhibits large amplitudes, with peak intensities of 30 mV/m in the 2.5 kHz band near 5 R_E, and peak intensities near 8–10 mV/m in the 600 Hz band near 8 R_E. We stress that these "maximum values" have still been averaged over four seconds; instantaneous amplitudes can greatly exceed these four-second averages, as will be shown in section 3.

[9] The magnetic component of the waves can be measured directly by the SCM, or can be inferred indirectly from the electric field amplitudes by assuming parallel propagation and a cold plasma dispersion relation [e.g., *Meredith et al.*, 2003]. Assuming typical parameters for the cyclotron and plasma frequencies, the mean electric field amplitudes of 1–2 mV/m translate to magnetic amplitudes of roughly 10–30 pT, while the maximum four-second averaged values of 8–30 mV/m translate to roughly 100–400 pT. Although a thorough analysis of the SCM data is outside the scope of this paper, these values are consistent with SCM filter bank data when binned in a similar manner.

[10] The geophysical role of these large-amplitude waves depends on the probability distribution of the wave amplitude, which is shown in the histograms in the rightmost plots of Figure 1. Data for these three histograms has been selected from the three regions shown. The probability distribution for 2.5 kHz in the dawn sector near 5 R_E (bottom plot, black) is particularly interesting; although the distribution is exponentially bounded (and hence not heavy-tailed in the formal sense), a substantial fraction of the total probability is contained in the tail of the distribution. The median and mean values for the wave amplitude in this region are only 0.03 and 0.4 mV/m respectively, while the probability of observing waves with four-second averaged amplitudes larger than 4 mV/m (i.e. an order of magnitude greater than the mean) is 2.5%.

[11] During most of 2007, the filter banks used AC-coupled data from the EFI instrument with a measurement range of ±80 mV/m at 1 kHz. Consequently, the largest-amplitude waves saturate the data stream. This effect will tend to truncate the tail of the distribution and reduce the maximum values (middle plots of Figure 1). For the 2008

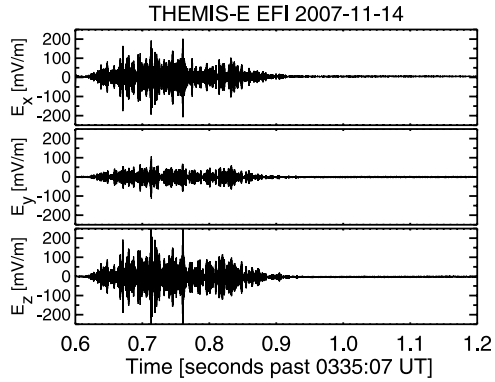

Figure 2. Three component EFI electric field data in GSM coordinates. The sampling rate is 8192 Hz, and the L-shell value is 4.3.

season, we may use DC-coupled data with a saturation threshold of 500 mV/m.

3. High-Resolution Waveforms

[12] The EFI also captures waveform data at rates up to 16 kS/s during short burst intervals, some of which were scheduled to coincide with the radiation belt encounters. The burst data give brief snapshots of the waveforms that are averaged into the filter bank data in section 2.

[13] In regions of low-amplitude waves, the wave power may be relatively steady over the four-second interval, in which case the filter bank value gives a good representation of the wave amplitude. However, in regions of high-amplitude waves, the burst waveforms present a very different picture. Instead of relatively constant wave amplitudes, the amplitude fluctuates dramatically over several orders of magnitude. Such intermittent, bursty signals are not well represented by the four-second averaged filter bank data.

[14] The burst of wave power in Figure 2 was captured by THEMIS E at L = 4.3, and is a particularly extreme example of an intense burst embedded in an otherwise relatively quiet environment. The burst lasts for about 0.3 seconds, with a peak amplitude reaching over 300 mV/m. The burst is extremely isolated; the filter banks report a four-second averaged amplitude of only 0.4 mV/m. However, the longer interval surrounding this burst shows enhanced wave activity, with filter bank values in the 10 minutes before and after varying over a wide range from 0.05 to 5 mV/m.

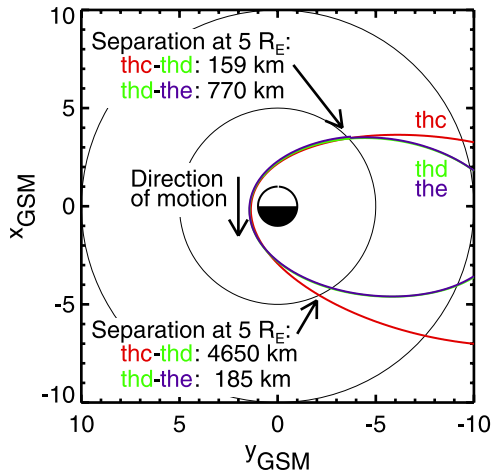

Figure 3. Orbits for THEMIS C, D and E on 16 November 2007. The orbits for THEMIS D and E are extremely similar, and are difficult to distinguish in the plot. Inbound and outbound legs are separated by 6.7 hours local time.

[15] The data in Figure 2 has been corrected by both deconvolving the instrument response and correcting for the effective boom lengths. However, the waves were near the Nyquist frequency for the 8192 Hz sampling rate; some of the signal is therefore aliased from higher frequencies, and the signal amplitude therefore underestimated. Based on the (1 kHz) bandwidth of the observed (aliased) signal, the power at 4–6 kHz in the onboard power spectra and the analog filter characteristics, the amplitude is underestimated by at most a factor of 40%, and more likely 10 to 20%.

4. Spatial and Temporal Extent of Large-Amplitude Waves: A Case Study

[16] Between 13 and 18 November 2007, the THEMIS satellites encountered regions of enhanced whistler wave power (filter bank values greater than 1 mV/m) on multiple passes. At this time, THEMIS D and E had nearly identical trajectories (Figure 3), while THEMIS C had a higher apogee at a slightly shifted local time.

[17] Wave power in the 2.5 kHz band was minimal on 12 November, but starting on 13 November, power began to build on the outbound legs. Amplitudes on the outbound leg remained high during passes on 13–14 November, and then diminished on 15 November (Figure 4a). Starting on

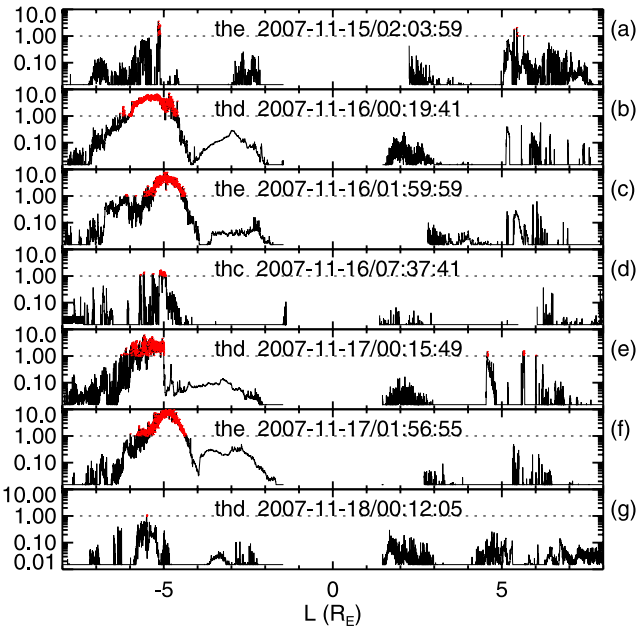

Figure 4. Filter bank amplitude in the 2.5 kHz band as a function of magnetic equatorial radius L. The inbound leg of each orbit has been assigned L < 0 to distinguish it from the outbound leg. Plots are arranged chronologically. Values below 0.015 mV/m have been plotted at 0.015 mV/m to distinguish low amplitudes from data gaps.

16 November, wave power then began to build on the inbound leg (Figures 4b–4f), reaching high and sustained values through 17 November before returning to low values on 18 November (Figure 4g).

[18] In total, 85 brief burst-mode waveforms were captured in the radiation belts during the interval between 13–17 November 2007. Although the largest observed amplitudes occur in the burst data shown in section 3, large-amplitude waves (many tens to hundreds of mV/m) appear repeatedly in the other bursts when nearby filter bank values are larger than about 1 mV/m. In association with the filter bank data in Figure 4, showing a persistent region of enhanced wave power, we conclude that regions of large-amplitude whistlers can persist in a similar location for days.

[19] By comparing the various passes in Figure 3, we can roughly estimate the size of the region of enhanced whistler power. First, enhanced power (>1 mV/m) is seen on the inbound leg (13–14 November, not shown) or on the outbound leg (Figures 4b, 4c, 4e, and 4f) but not both. Thus, the waves are azimuthally localized to at most 6 hours of local time, and do not cover the whole dawn sector simultaneously. Also, although probes D and E observed similar large amplitudes on both 16 and 17 November (Figures 4b, 4c, 4e, and 4f), probe C saw substantially smaller signals (Figure 4d). Since the outbound leg of probe C was separated from those of D and E by only 0.5 hours local time, we conclude that the regions of large-amplitude waves have well-defined edges. Since it seems unlikely that THEMIS D and E would encounter the region so repeatedly if it were extremely small, we conclude that the region of intense emissions is localized, with an azimuthal extent between 1 and 4 hours in local time. The radial extent ($\sim$1 R_E) is dictated by the measurement frequency band (1.3 to 3.7 kHz) and has little geophysical meaning; at larger distances, the electron cyclotron frequency is lower, so that the upper whistler band no longer falls in the range of the bandpass filter.

[20] Advanced Composition Explorer (ACE) data for the relevant dates show an interval of high speed solar wind (600 km/s) starting on 13 November 2007. Geomagnetic activity was low to moderate, likely due to a fluctuating z component of the interplanetary magnetic field. The THEMIS ground-based magnetometer array observed a number of substorms and smaller disturbances, but no major events. The provisional AE index was quiet to moderate, the Kp index remained at or below 3+, and the provisional DST index was quiet, with no excursions below −30 nT over the interval in Figure 4. These conditions (high-speed solar wind, low to moderate geophysical activity) have been linked with effective radiation belt particle acceleration [*O'Brien et al.*, 2001; *Onsager et al.*, 2007] and increased whistler-mode chorus emissions [*Hwang et al.*, 2007].

5. Conclusions

[21] The THEMIS filter bank data can be used to paint a broad picture of wave activity in the inner magnetosphere. Using the four-second averaged data, the average amplitude of whistler waves in the chorus region (dawn sector, L = 4–8) is several mV/m, consistent with previous results [*Meredith et al.*, 2001]. However, the probability distribution of the wave amplitudes has significant probability far out into the tail, which makes average values potentially misleading. The distribution of several kHz power near L = 5 has a particularly "heavy" tail, with 2.5% of the samples having an amplitude greater than an order of magnitude larger than the mean.

[22] Burst data show that there are still greater wave amplitudes than those seen in the four-second averaged filter bank data. Waves with amplitudes >100 mV/m are observed, and are usually confined to short-duration packets which tend not to show up in four-second averages.

[23] Large-amplitude waves are observed in a localized region with a long lifetime. The case study presented time-averaged wave amplitudes of roughly 10 mV/m in the 2.5 kHz band, with bursts to several hundred mV/m. The region of enhanced activity persisted for several days, and was localized to an azimuthal extent of several hours. The region wandered in azimuth over several days, appearing first near 02 local time, and then later near 09 local time.

[24] Whistler waves with amplitude >100 mV/m can dramatically accelerate electrons in their vicinity. Much of the previous work on the mechanisms and rates of relativistic electron acceleration via dawn chorus [e.g., *Horne et al.*, 2005, and references therein] has used time-averaged spectral densities which may not be fully representative of the true conditions, as discussed above. With large regions of space covered by bursty, large-amplitude waves, the actual mechanisms and rates may be qualitatively or quantitatively different.

[25] **Acknowledgments.** This research was funded by NASA contract NAS5-02099 (THEMIS). The THEMIS project has been made possible by many individuals whom we thank greatly, in particular V. Angelopoulos and F. Mozer. We acknowledge the WDC for Geomagnetism, Kyoto University, Japan for the geomagnetic indices, and D. J. McComas, N. Ness and CDAWeb for the ACE data.

References

Angelopoulos, V. (2008), The THEMIS mission, *Space Sci. Rev.*, in press.

Cattell, C., et al. (2008), Discovery of very large amplitude whistler-mode waves in Earth's radiation belts, *Geophys. Res. Lett.*, *35*, L01105, doi:10.1029/2007GL032009.

Elkington, S. R., M. K. Hudson, and A. A. Chan (2003), Resonant acceleration and diffusion of outer zone electrons in an asymmetric geomagnetic field, *J. Geophys. Res.*, *108*(A3), 1116, doi:10.1029/2001JA009202.

Horne, R. B., and R. M. Thorne (2003), Relativistic electron acceleration and precipitation during resonant interactions with whistler-mode chorus, *Geophys. Res. Lett.*, *30*(10), 1527, doi:10.1029/2003GL016973.

Horne, R. B., R. M. Thorne, S. A. Glauert, J. M. Albert, N. P. Meredith, and R. R. Anderson (2005), Timescale for radiation belt electron acceleration by whistler mode chorus waves, *J. Geophys. Res.*, *110*, A03225, doi:10.1029/2004JA010811.

Hwang, J. A., D.-Y. Lee, L. R. Lyons, A. J. Smith, S. Zou, K. W. Min, K.-H. Kim, Y.-J. Moon, and Y. D. Park (2007), Statistical significance of association between whistler-mode chorus enhancements and enhanced convection periods during high-speed streams, *J. Geophys. Res.*, *112*, A09213, doi:10.1029/2007JA012388.

Li, X., M. Temerin, D. N. Baker, G. D. Reeves, and D. Larson (2001), Quantitative prediction of radiation belt electrons at geostationary orbit based on solar wind measurements, *Geophys. Res. Lett.*, *28*(9), 1887–1890.

Mann, I. R., T. P. O'Brien, and D. K. Milling (2004), Correlations between ULF wave power, solar wind speed, and relativistic electron flux in the magnetosphere: Solar cycle dependence, *J. Atmos. Sol. Terr. Phys.*, *66*, 187–198.

Meredith, N. P., R. B. Horne, and R. R. Anderson (2001), Substorm dependence of chorus amplitudes: Implications for the acceleration of electrons to relativistic energies, *J. Geophys. Res.*, *106*(A7), 13,165–13,178.

Meredith, N. P., M. Cain, R. B. Horne, R. M. Thorne, D. Summers, and R. R. Anderson (2003), Evidence for chorus-driven electron acceleration to relativistic energies from a survey of geomagnetically disturbed periods, *J. Geophys. Res.*, *108*(A6), 1248, doi:10.1029/2002JA009764.

O'Brien, T. P., R. L. McPherron, D. Sornette, G. D. Reeves, R. Friedel, and H. J. Singer (2001), Which magnetic storms produce relativistic electrons at geosynchronous orbit?, *J. Geophys. Res.*, *106*(A8), 15,533–15,544.

Omura, Y., N. Furuya, and D. Summers (2007), Relativistic turning acceleration of resonant electrons by coherent whistler mode waves in a dipole magnetic field, *J. Geophys. Res.*, *112*, A06236, doi:10.1029/2006JA012243.

Onsager, T. G., J. C. Green, G. D. Reeves, and H. J. Singer (2007), Solar wind and magnetospheric conditions leading to the abrupt loss of outer radiation belt electrons, *J. Geophys. Res.*, *112*, A01202, doi:10.1029/2006JA011708.

Santolk, O., D. A. Gurnett, J. S. Pickett, M. Parrot, and N. Cornilleau-Wehrlin (2003), Spatio-temporal structure of storm-time chorus, *J. Geophys. Res.*, *108*(A7), 1278, doi:10.1029/2002JA009791.

Summers, D., and Y. Omura (2007), Ultra-relativistic acceleration of electrons in planetary magnetospheres, *Geophys. Res. Lett.*, *34*, L24205, doi:10.1029/2007GL032226.

J. W. Bonnell, Space Sciences Laboratory, University of California, Berkeley, CA 94720-7450, USA.

C. M. Cully, Swedish Institute of Space Physics, Box 537, SE-751 21 Uppsala, Sweden. (chris@irfu.se)

R. E. Ergun, Laboratory for Atmospheric and Space Physics, University of Colorado, Boulder, CO 80303, USA.